



Geophysical research applied to the evaluation of percolation conditions of an earth dam

Luiz Filipe Caríssimo Soares¹ · Cibele Aguiar Cláuver² · Lais Brenda Lopes Rezende¹ · Eduardo Antonio Gomes Marques²

Received: 1 November 2023 / Accepted: 10 July 2024 / Published online: 2 August 2024
© The Author(s) 2024

Abstract

Safety conditions in geotechnical structures require the investigation of the phenomena responsible for the loss of their stability. When combined with commonly used direct investigations, geophysical methods add greater efficiency to geotechnical investigations, since their application allows the acquisition of a large amount of data in a short period of time, and at a relatively low cost. In this context, the present study aimed to evaluate percolation through the massif of a small earth dam, based on an integrated interpretation of results obtained with the application of the geophysical methods of Electroresistivity and Self Potential, in addition to results from geotechnical investigations previously carried out on the structure. The results proved the efficiency of the proposed methodology, allowing the confirmation of hypotheses formulated by other authors in previous studies of the same dam. Also, the results allowed the evaluation of the efficiency of correction works carried out in the dam massif to solve the problems caused by a piping process. Among the identified geotechnical properties, a preferential flow path, which indicates the occurrence of a water loss process through the dam foundation layer, was detected and can be linked to the occurrence of a landslide on the downstream slope of the embankment. It can be concluded that the geophysical survey effectively evaluated the geotechnical conditions and seepage within the massif and its foundations, meeting the study's objectives. Both shallow and deep flow paths in the study area were delineated, pinpointing the factors contributing to their occurrence.

Keywords Geophysical investigation · Earth dams · Seepage · Integrated interpretation

Introduction

The construction of earth and rockfill dams is among the oldest activities carried out for the benefit of human communities, with the first examples of such structures having been built since a few millennia ago (Kutzner 1997). In Brazil, small earth dams are built for various purposes, such as human supply, agricultural exploitation and flood regulation (ANA 2016).

Given the socio-economic importance of these structures and the potential for human and material losses and

environmental damage that may result from their failure, the assessment of flow conditions in massifs of earth dams is a matter of great interest and relevance for both the community and the general population.

An example of a structure whose failure can have severe impacts on the surrounding community is a small earth dam located in the city of Viçosa, Brazil. The dam has the function of storing water for human supply, and in July 2022 a partial failure was recorded on the downstream slope, close to the right abutment.

The failure mechanisms commonly associated with the presence of water in the massif of earth dams include piping, which consists of a form of internal erosion that results in the emergence of preferential flow paths in the massif due to the lack of control of percolation (Fell and Fry 2007; Robbins and Griffiths 2018) and the phenomenon of liquefaction, which is associated with the generation of excessive pore pressures in sandy soils in the loose state (Casagrande 1976).

✉ Luiz Filipe Caríssimo Soares
luiz.carissimo@ufv.br; luizfilipe.carissimo@hotmail.com

¹ Graduate Program in Civil Engineering, Federal University of Viçosa, Viçosa, State of Minas Gerais, Brazil

² Department of Civil Engineering, Federal University of Viçosa, Avenida Peter Henry Rolfs, University Campus, Viçosa, State of Minas Gerais CEP 36570-900, Brazil

Ongoing monitoring activities are the most effective practice for managing safety and operating conditions in earth dams. Several procedures were developed to investigate and monitor the geotechnical and geological characteristics of the embankments, such as the execution of percussion drilling and the installation of water level meters, piezometers and inclinometers (Kutzner 1997; Cruz 2004). In a complementary way, geophysical methods can be applied as an efficient practice to investigate the internal structure of soil or rock masses, allowing the acquisition of a large volume of data, relatively quickly and non-invasively, and which is applicable in steep areas that are hard to reach by equipment used in conventional investigation (Jongmans and Garambois 2007; Kearey et al 2009). In addition, parameters measured during geophysical investigations jointly reflect the geological and hydrological characteristics of the underground material, which sometimes cannot be identified separately (Pazzi et al. 2019). In this context, for investigations in earth dams, geophysical methods studying the properties of the electric field in the subsurface, such as Electrical Resistivity and Spontaneous Potential methods, are intensively applied.

The Electrical Resistivity (ER) method is an active method, in which an electrical signal is transmitted in the subsurface. The property calculated from the measurements of electrical properties of the underground materials is the electrical resistivity, which is related to the difficulty encountered by the electrical current to propagate through a given medium. Since the minerals forming rock matrices are generally worse electrical conductors than water, the resistivity of soils and rocks is influenced by the presence of water in their pores, which acts as an electrolyte. Thus, resistivity in sedimentary media depends on the porosity of the material, the fraction of pores filled with water (saturation) and the type and concentration of ions dissolved in water, among others (Lowrie 2007; Dentith and Mudge 2014).

The most common applications of ER surveys in earth dams include the delimitation of contact zones between materials with different electrical resistivity (Cardarelli et al. 2010; Grangeia et al. 2011), the mapping of the water table (Bedrosian et al. 2012; Rocha et al. 2019) and the detection of preferential flow paths through the massif (Bièvre et al. 2017; Camarero and Moreira 2017; Raji and Adedoyin 2019; Franco et al. 2024). These features are usually associated with regions showing anomalous resistivity bands in relation to their surroundings.

Raffek (2016) underscores the dependence of soil resistivity on the amalgamation of its three phases (solid, liquid, and gas). The resistivity of the liquid phase correlates with its ionic concentration, while grain resistivity is contingent upon surface electric charges, with air serving as an insulating agent. Regarding the measurement of resistivity in anisotropic media, both the ratio and geometric alignment

of constituent materials exert an influence on the resulting resistivity value. For example, laminar structures exhibit variable resistivity when assessed parallel or perpendicular to the direction of laminations (Reynolds 2011). Telford et al. (1990) suggest that in heterogeneous environments, the apparent resistivity of the medium is ascertained, approximating the true resistivity of the area. However, this apparent resistivity value does not merely reflect an arithmetic average of the resistivities of the materials comprising the subject medium.

On the other hand, the Self Potential (SP) method is based on the natural potential that can be measured between two electrodes coupled to the surface, without the application of an artificial electric field (Corwin 1990). The main mechanism responsible for generating spontaneous potential signals in earth dams is the electrokinetic (flow) potential, which occurs from the flow of water in a porous medium. Anions are absorbed by the soil capillary network, forming an electrical double layer, while cations are carried by the water flow, generating a higher concentration of positive ions downstream (Gallas 2005).

The most common application of SP surveys in earth dams is the detection of infiltrations in the massif, which can indicate internal erosion (Panthulu et al. 2001; Bolève et al. 2011; Netto et al. 2020). This phenomenon is generally associated with the occurrence of negative SP anomalies downstream.

In order to obtain more precise interpretations of data acquired by geophysical methods, these results can also be analyzed together with geological data collected in the field in the study area (Andrades-Filho et al. 2014; Medeiros and Córdoba 2020). This methodology can also be used to elucidate ambiguities that may arise in the interpretation of geophysical data (Roy 1962; Golebiowski et al. 2016), thus, the combination of different approaches in the investigation, based on the different methods available, can help in obtaining more reliable results (Telford et al. 1990).

In this context, the objectives of the study were to evaluate seepage conditions and the origin of piping in a small earth dam, and its possible connection with a failure in the embankment after the survey was performed. The geophysical methods of Electroresistivity (ER) and Self Potential (SP) were applied in this survey, together with available data from percussion drilling (SPT) performed on site and laboratory tests.

Site description

Location and description of the dam

The dam is located in the municipality of Viçosa, state of Minas Gerais, Brazil, inside the campus of the Federal

University of Viçosa (Fig. 1). It is a small earth dam, built as an uncontrolled compacted embankment, without an internal drainage system, with water storage function (Fig. 2). A concrete spillway was installed on the crest of the dam, while another spillway, with a larger cross section, was excavated on the right bank of the reservoir and partly covered by grass and partly by concrete, coming into operation only in periods of heavy rains. There are no records of when the structure was built, nor of geophysical surveys previously carried out at the site.

Prior to the geophysical investigation, a process of water loss from the reservoir through the foundation layer of the dam was detected, while an erosion cavity, resulting from a piping process, was identified on the downstream slope of the dam massif, close to the concrete spillway (Minette 2015). Emergency interventions were made to prevent the collapse of the structure (Fig. 3).

Description of the local geology

The dam area has a predominantly strong undulating mountainous relief, with a convex-concave slope with flat-bottomed valleys, formed by terraces and larger beds,

where small streams flow (Corrêa, 1984). The predominant rock is gneiss, with varied texture, found in different degrees of weathering alteration. Other high-grade metamorphic rocks, such as amphibolites and migmatites may also occur (Daker 1983; Andrade 2010).

The study area, however, does not have rocky outcrops. Quaternary sediments, which are characterized by high textural variety, occur along the valleys (Marques 2008). Such that it is reflected in the context of the dam itself, the hydrogeology of the area is represented by a porous, unconfined aquifer, formed by Quaternary alluvial deposits and residual gneiss soils (Rocha 2015).

A report from a percussion drilling (SPT) in the dam carried out in 2018 showed three main geological layers, without determining the depth of the bedrock (Fig. 4), due to limitations in the equipment applied during the investigations. The backfill layer of the dam has a texture varying between sandy silt and red silty clay, with mica, approximately 6 m thick. The foundation layer is composed of alluvial material with a texture ranging from fine to medium sand, with the presence of organic matter, mica and gravel. Below is the residual gneiss soil layer (Universidade Federal de Viçosa 2018; Dalmascio et al. 2019).

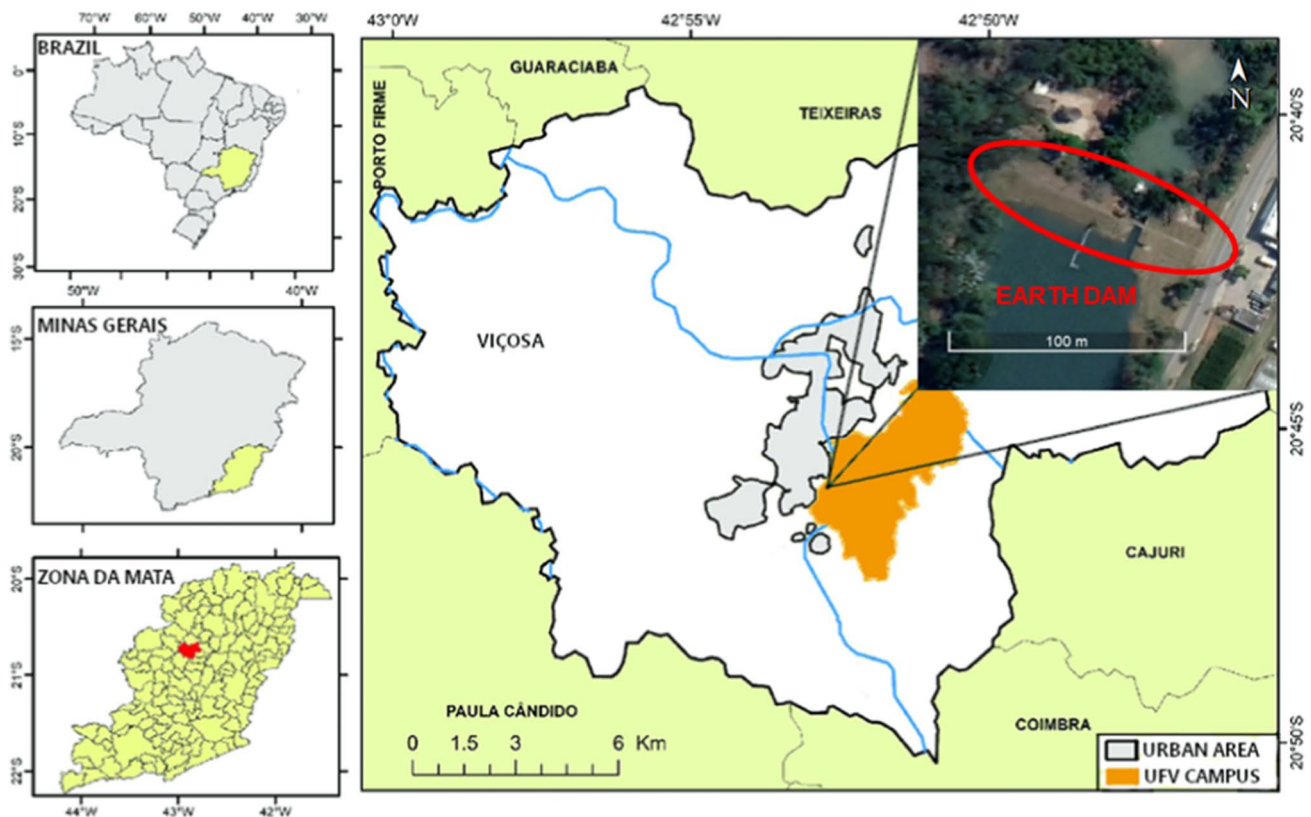
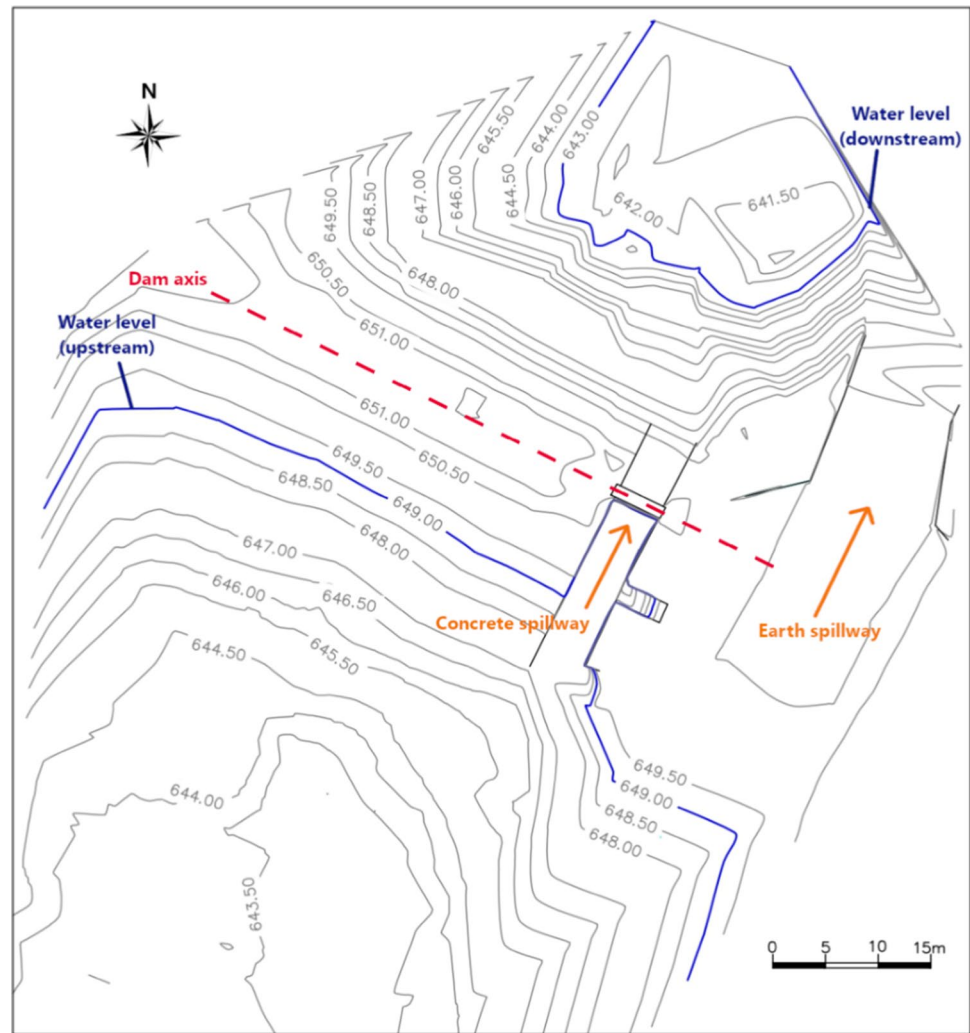


Fig. 1 Location of the study area (adapted from Avila-Diaz et al. 2020)

Fig. 2 Detailed view of the contour lines and structures present on the dam (adapted from UFV 2018)



Geophysical survey

A geophysical survey was carried out in order to characterize the materials on the subsurface of the embankment, using the ER and SP methods. This section of the work describes the data acquisition and processing techniques used to obtain the results presented later.

Survey setup

Prior to data acquisition, the massif was visually inspected. This procedure aimed to verify the structural integrity of the dam, as well as the identification of objects and structures present in the massif that could generate interference or anomalies in the results of the geophysical survey.

Several PVC pipes that are part of the water abstraction system of the reservoir were identified on the dam crest, and the presence of large anthills and large trees on the downstream slope can be observed (Fig. 5). No evidence of problems, such as cracks and erosive cavities, were identified in

the dam massif. In the place where the erosive cavity generated by the piping process (downstream slope, Fig. 3) was previously identified, no water surge was observed on the surface, indicating that the water flow was properly stemmed at the time of visual inspection.

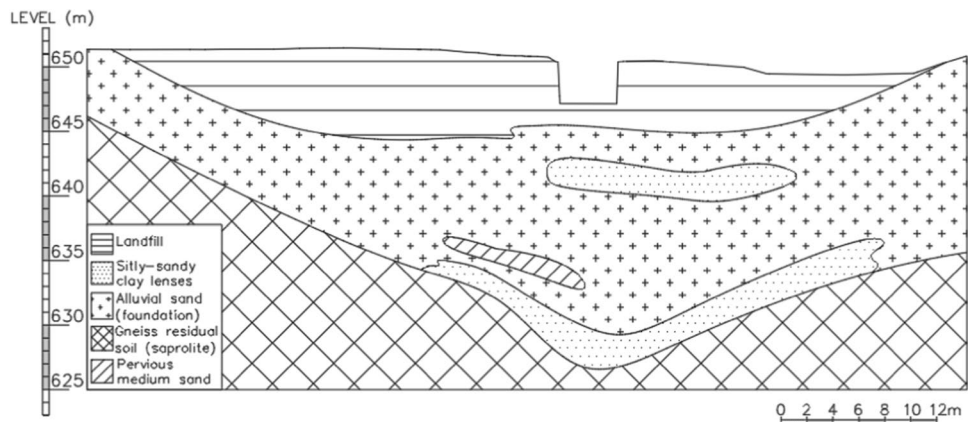
Important to notice that field data were collected in December 2019, during a period of intense rains, which influenced the results obtained. A total rainfall of 206.4 mm was recorded during the two weeks prior to data acquisition (UFV 2021).

The positioning of line profiles for the execution of the geophysical survey was determined after visual inspection. Five lines were delimited, covering the crest, upstream and downstream slopes of the embankment. The goal was to cover largest possible portion of the study area, as well as all the interest points that were observed during the performing of the visual inspection (Fig. 6 and Table 1). Parallel profiles were adopted due to the small size of the dam, thus, the short distance between the lines did not generate significant data loss.

Fig. 3 Location and detail of the erosive cavity caused by piping on the downstream slope (adapted from Minette 2015)



Fig. 4 Geological longitudinal cross-section of the embankment (adapted from UFV 2018)



SPT

To correlate the results of geophysics with more traditional tests, existing data from Standard Penetration Tests (SPT) conducted in 2019 were utilized. The selected points for the tests were boreholes 1 to 5, as depicted in Fig. 7, which provides a plan view of the massif.

The Standard Penetration Tests (SPT) were conducted concurrently with permeability tests following the guidelines outlined in NBR 6484:2001, which prescribe the method for performing basic soil exploration boreholes. This allowed for the development of cross-sectional and longitudinal profiles of the dam in the direction of borehole alignment.

Survey by the ER method

In geoelectrical explorations, a key aspect under scrutiny is the electrical resistivity, which mirrors the challenge encountered by an electrical current in traversing a given medium. Consequently, electrodes are strategically positioned to capture the current's pathway, as the flow of electric current in sediments and rocks heavily relies on ion migration through water situated within interconnected pores, acting as conductors (ABGE 1998).

In this study, the techniques for gauging electroresistivity entail a setup featuring four electrodes. Two electrodes (A and B) facilitate the transmission and receipt of electric



Fig. 5 Large trees and anthills and PVC pipes spotted during the visual inspection stage

Fig. 6 Line profiles adopted for the geophysical survey



Table 1 Description of the line profiles

Profile	Length (m)	Position	Start point			End point			Distance from the previous profile (m)
			N	E	Level (m)	N	E	Level (m)	
L01	53.00	Downstream slope	7,702,315.88	721,743.09	648.18	7,702,288.87	721,787.52	650.83	-
L02	53.00	Downstream slope	7,702,314.01	721,741.95	649.21	7,702,286.64	721,786.48	650.88	2.13
L03	93.00	Downstream slope	7,702,333.19	721,706.08	653.02	7,702,284.77	721,784.70	650.74	2.69
L04	90.00	Crest	7,702,324.77	721,704.84	652.51	7,702,283.82	721,785.16	650.86	8.90
L05	89.00	Upstream slope	7,702,319.96	721,703.42	652.66	7,702,279.39	721,782.80	650.84	5.16

UTM zone: 23 S

current (I) into the soil, while the remaining pair (M and N) measure the potential difference (ΔV) between them.

Investigation by the ER method was carried out from the application of the Electrical Resistivity Tomography (ERT)

along the five lines defined in Sect. 3.1. In this technique, a pair of electrodes is used to introduce the artificial electric current into the subsurface, at a fixed position, while another pair of electrodes, used to measure the potential variation,

Fig. 7 SPT Borehole locations

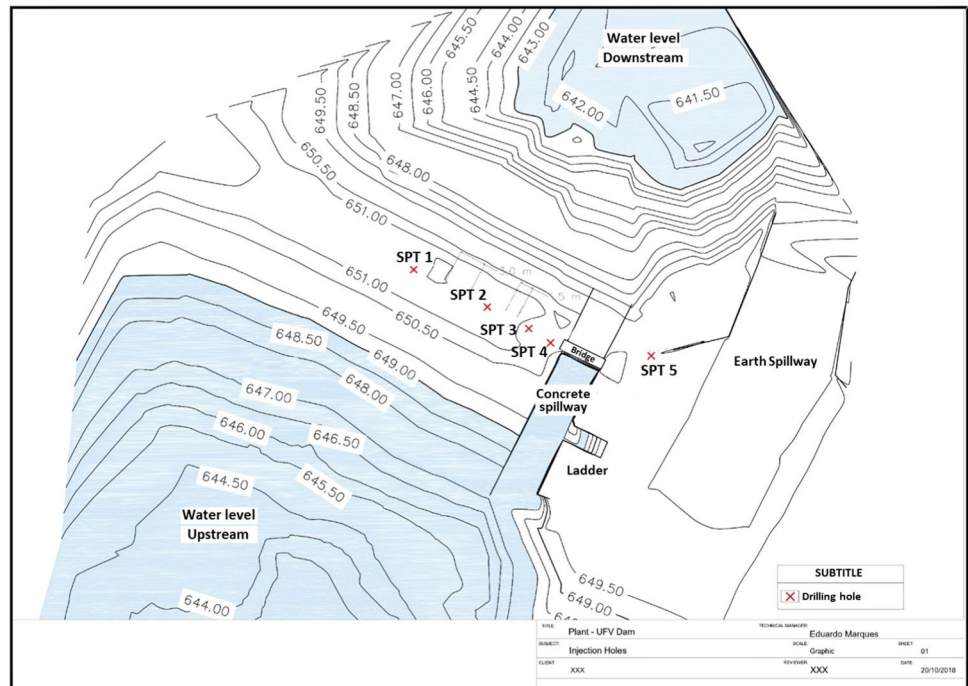


Table 2 Summary of the electrodes used on each profile

ID	Number of electrodes	Spacing between electrodes
L01	54	1 m
L02	54	1 m
L03	96	1 m
L04	92	1 m
L05	91	1 m

is moved along the lines, maintaining a fixed spacing, and the apparent resistivity value is calculated (Kearey et al. 2009; Reynolds 2011). The summary of the electrodes used on each profile and the electrode spacing is presented in Table 2.

The equipment used for the ERT was the Super Sting R8 IP resistivimeter, manufactured by Advanced Geosciences Inc., connected to a switch box that automatically moved the electrode array, and a set of metal electrodes embedded in the ground surface, with the number of electrodes varying with the length of each profile. A combination of dipole–dipole and gradient arrangements was adopted for the execution of ERTs, keeping a spacing of 1 m between the electrodes. This arrangement has a good signal-to-noise ratio and a good horizontal resolution for resistivity variation (Gandolfo 2007), being suitable for the detection of anomalies along geological layers of the massif.

Data were processed using the RES2DINV software, produced by Geotomo Software. The software was employed

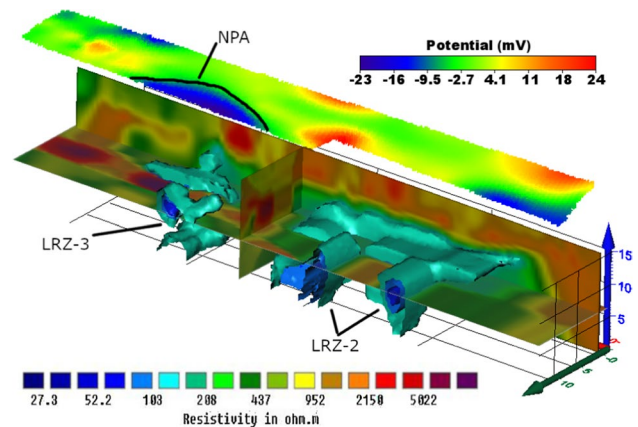


Fig. 8 3D view of the resistivity and self-potential data

to perform the inversion process on the apparent resistivity data, applying an iterative finite element model, which was modified until the difference between the measured and calculated data was below an acceptable limit.

A 3D model for the distribution of the resistivity values is showed in Fig. 8. This model was created using the software *Voxler*, produced by GoldenSoftware. It is imperative to note that the resultant image attains the pinnacle of resolution and quality achievable within the constraints of *Voxler's*, which were limited by the equipment available at the time. This contrasts with software like *EarthImager*, as leveraged by Franco (2024), which may offer higher capabilities. However, regrettably, such alternatives were not accessible to us

during the study. The software *Voxler* produced a gridding model, applying the Inverse distance to a power method. In this process, data are weighted during interpolation such that the influence of a point datum declines with distance from the lattice node, and then resistivity value was determined in the space between the profiles.

Survey by the SP method

In the study of seepage, the main mechanism responsible for generating flow potentials is called electrokinesis (Gallas 2005), in which cations are transported, creating a positive potential gradient through the downstream direction.

Investigation by the SP method was carried out along the same line profiles as shown in Fig. 6. Data were acquired using the fixed-base configuration, in which the potential value is measured between a stationary electrode and an electrode that is moved along the survey lines. This configuration was chosen for its easy application and for presenting low cumulative errors (Corwin 1990). The stationary electrode was positioned on the dam crest, close to the L04 line, while the mobile electrode was attached to the ground surface, keeping a spacing of 3 m between each measurement point. At the beginning and end of the readings in each line, the potential was measured at a point close to the fixed electrode, to compensate electrode polarization effects that may occur during data acquisition.

The equipment used was the SAS 1000 resistivimeter, manufactured by ABEM, and a pair of non-polarizable copper sulfate (CuSO₄) electrodes coupled to the surface. Data were processed in Microsoft Excel software, which was used to correct electrode polarization that occurred during data acquisition. Surfer software, produced by Golden software, was used to create a 2D model of the distribution of potential values along the study area. To this end, the software applies

a kriging process to the data, which is an interpolator in which the influence of the measured punctual data decreases with the distance to the calculated node.

It is important to note that the ER and SP surveys were carried out on the same profiles in order to provide the redundancy of geophysical data using different methods which is necessary to obtain more accurate interpretations.

Results and discussion

The evaluation of geotechnical conditions and seepage through the dam are presented in this section. The integrated interpretation of the geophysical survey results, together with the available geotechnical data, is also discussed.

Standard penetration tests

The reports of the SPT tests are presented in Table 3, showing the blow count, the count of the blows in the first and last 30 cm of each 45 cm operation, Ground Water Table (GWT) depth and soil classification for each of the boreholes described in this paper.

Results of the ER survey

The results of the ER survey showed two high resistivity zones (HRZs) below the downstream slope. The first (Fig. 9c) is large in extent, starting approximately 2 m below the surface at line L03 (HRZ-1) extending between the dam massif and foundation layers (Fig. 10b). According to results of the SPT drilling carried out previously at the site, shown in Fig. 10b, this region has a low penetration resistance (SPT-5). This combination of results indicates that the portion of the soil delimited by HRZ-1 may be damaged, with a

Table 3 Summary of the SPT test results

Depth (m)	Borehole SP-01			Borehole SP-02			Borehole SP-03			Borehole SP-04			Borehole SP-05					
	Blow/30 cm		GWT (m)	Blow/30 cm		GWT (m)	Blow/30 cm		GWT (m)	Blow/30 cm		GWT (m)	Blow/30 cm		GWT (m)			
	5,70	First	Last	5,70	First	Last	5,33	First	Last	5,63	First	Last	2,82	First	Last			
01	10	13		14	17		06	06		07	08		04	06				
02	05	08		10	13		08	11		06	07		06	07				
03	13	14	Micaceous sandy silt	08	12	Micaceous sandy silt	08	09	Micaceous sandy silt	06	08	Micaceous sandy silt	05/34	08	Micaceous sandy silt			
04	06	10		09	10		08	09		06	07		02	04				
05	06/35	07		06	07		08	10		06	11		05	07				
06	06/34	07/34		03	06	Micaceous medium sand	09	12		09	09		04	04	Micaceous silty sand with alluvion			
07	07	08		05	06		14	14		08	09		04	04				
08	06	07	Micaceous silty sand with alluvion	07	09	Silty-clay	06	05	Micaceous silty sand with alluvion	09	11	Fine and medium dark sand with organic material	05/36	07				
09	04	05		09	10		04	04		03	05		02	03/34		03	07	Sandy-silty clay
10	04	05		11	13		12	16		04	10		04	10	02	03/35		
11	08	11		07	09	Micaceous fine sand	12	16		13	18		13	18	04/37	04/35		
12	04	04		07	08		12	14		13	15		04/35	03				
13	04	04		06	07		09	10		08	09		05	08				
14	05/34	04	Residual soil	08	08		09	09		07	07		09	12	Micaceous silty sand with alluvion			
15	04	06					07	10	05	07	03/40	03	03/39	02				
16						04/39	06/31	Medium sand		05	05		10	12				
17						04	05	Micaceous silty sand		03	05		05	05				
18						04/35	05/35	Sandy-silty clay					13	18				
19						06	08						05	07	Sandy-silty clay			
20						13	15	Residual soil					-	-				
21													10	20	Residual soil			
22																		

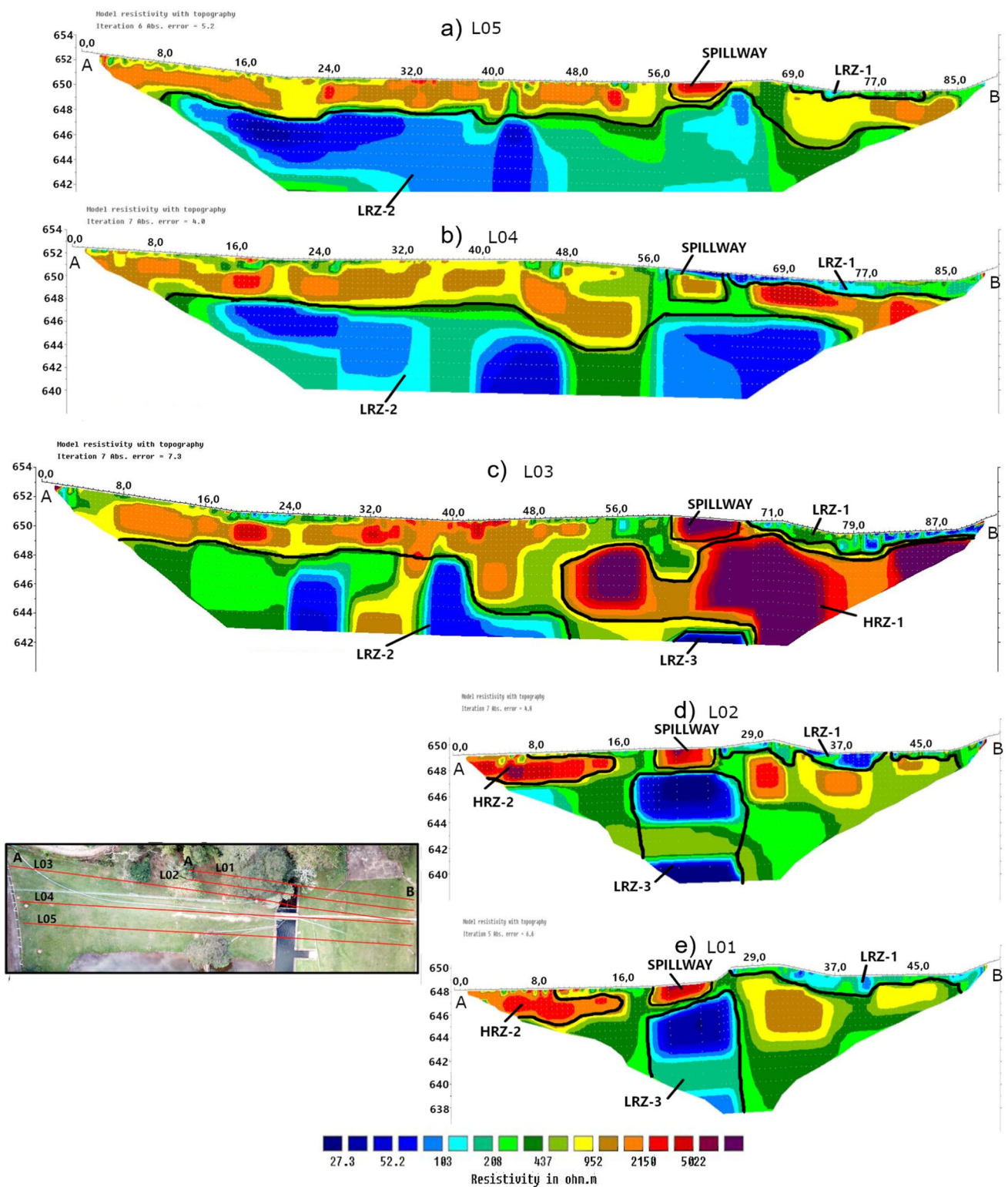


Fig. 9 Results from the ER survey

high void rate (Oh and Sun 2008), probably due to a poorly executed compaction process during the construction of the structure. Thus, high resistivity values can be explained by

the high resistivity of the air filling the voids in the soil, in relation to solid particles. The second HRZ is shallow and of small extent (HRZ-2), located in the same area where

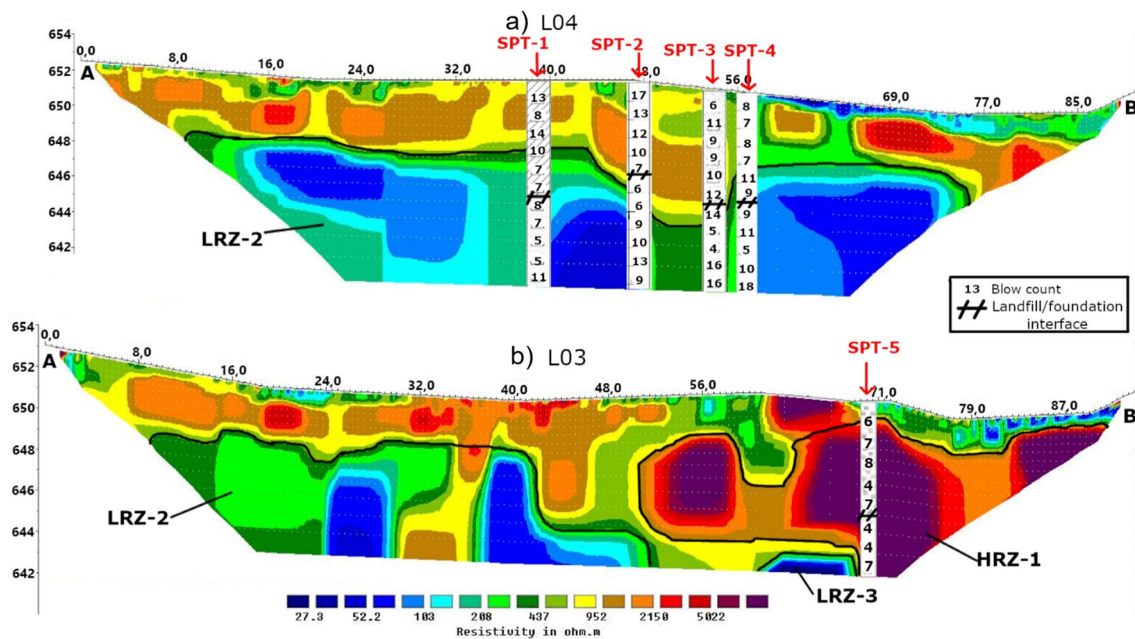


Fig. 10 Integrated results of the SPT and ER surveys

large anthills and trees were identified during visual inspection (Fig. 9d and 9e). These biological agents cause high resistivity values, as the growth of roots and the expansion of the anthill can damage the soil, increasing porosity (ANA 2016). Thus, the soil mass delimited by HRZ-2 is in a loose state, with most voids filled with air. The region corresponding to the location of the concrete spillway is also shown in Fig. 9. It is important to highlight that resistivity data were not measured along the spillway section, due to difficulties in reaching the spillway sill to couple the electrodes. Thus, the resistivity data shown in the region corresponding to the overflow section was generated during data processing to fill in the region with missing data in the resistivity profiles. Therefore, no geological property of the site should be inferred from their interpretation. Three low resistivity zones (LRZs) were identified in the results of the ER method. The first is shallow (LRZ-1), approximately 1 m thick, whose location coincides with the earth spillway on the right bank of the reservoir (Fig. 9a to 9e). Low resistivity values are associated with the intense rains occurring before the geophysical survey, since excess water from the reservoir flows through this spillway, causing an infiltration along its length. Thus, we interpreted that the soil mass delimited by the LRZ-1 represents an infiltration zone due to the dam configuration.

The second (LRZ-2) is a large area whose upper limit is approximately at an elevation of 649 m, extending between sections L03, L04 and L05 (Fig. 9a to 9c). The position of LRZ-2 is consistent with the water level of the reservoir, implying that its upper limit corresponds to the water table

inside the massif. The third zone is deeper, recorded in profiles L01, L02 and L03 (LRZ-3), and is located below the concrete spillway (Fig. 9c to e). We interpreted that this zone delimits a preferential percolation path, since it is located below the water table and has low resistivity values in relation to its surroundings.

Results of the SP survey

The results of the SP survey (Fig. 11) indicated two superficial flow zones (SFZs) along the surface of the dam, which have no correlation with water percolation inside the structure. The configuration of potential values in these regions is consistent with the electrokinetic mechanism, with the direction of the flow determined by the local topography, and the potential values increasing downstream, as indicated in Fig. 11. We interpreted that these shallow flow zones were identified due to heavy rains in the study area prior to data acquisition (December 17th–19th, 2021), which were registered by UFV (2021), as presented in Fig. 12.

Also, a negative potential anomaly (NPA) was identified on the downstream slope of the dam, recorded on profiles L01, L02 and L03. This anomaly is located around the concrete spillway, and considering that the subsurface flow through the massif occurs perpendicular to the dam axis, it was associated with an intense cation displacement that may have been caused by a subsurface infiltration.

Fig. 11 SP survey results

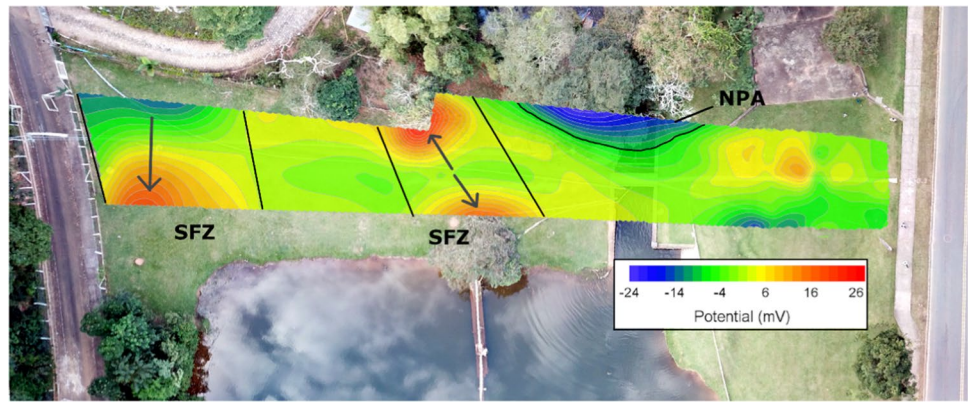
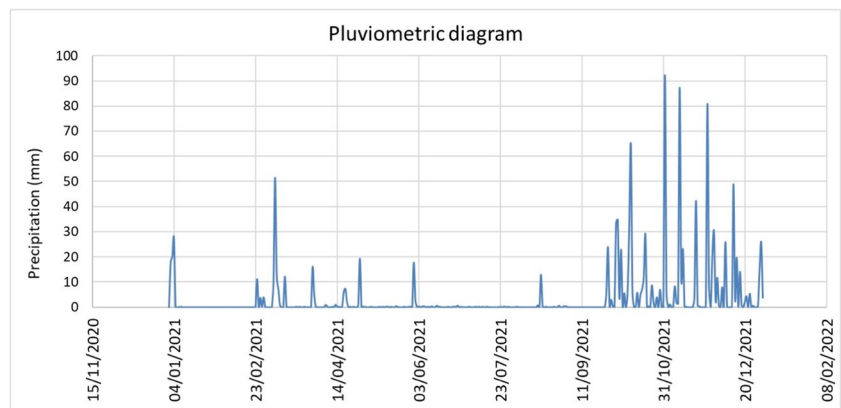


Fig. 12 Pluviometric Diagram registered in 2021 at the study area



Preferential flow paths and infiltration detection

From the integrated interpretation of the geophysical survey results and the available geotechnical data, we identified preferential flow paths through the massif. The 3D model for the distribution of the resistivity values showed in Fig. 8 was obtained as described in Sect. 3.2. The two deep LRZs identified in the ER survey results are highlighted in the model.

Considering that the water flow direction is perpendicular to the dam axis, the LRZ-2 delimits the subsurface region in which water percolation occurs with more intensity, due to low resistivity values in relation to its surroundings. From the results of the SPT drilling and considering that the water table level is associated with the upper limit of LRZ-2, we interpreted that this region is located almost entirely in the foundation layer, thus percolation occurs preferentially under the structural embankment.

The distribution of potential values obtained from the results of the SP survey is also presented in Fig. 8. Both the NPA and the LRZ-3 were recorded in the same profiles, and these two features have similar positions in the massif, and it is possible to infer that this correlation indicates a process of water loss through the foundation layer of the dam, in the region below the concrete spillway. The occurrence of this infiltration is consistent with the abrupt lowering of

the water level observed in profile L3 by the ER method, indicating the existence of a sink in the alluvial sand layer. High resistivity values recorded in HRZ-1 are also consistent with the lowering of the water table, as these values can be associated with voids filled with air in the soil mass delimited by HRZ-1. Therefore, the convergence of the results presented here indicates the existence of a critical region, with an infiltration process responsible for the emergence of the preferential flow path delimited by LRZ-3, confirming the reports of previous studies on the loss of water from the reservoir.

Connection of the geophysical results with the occurrence of a landslide on the embankment

In July 2022, after the acquisition and interpretation of the geophysical data, a landslide occurred on the downstream slope of the dam, between the two spillways. This was a partial failure, which did not lead to the total collapse of the embankment. As shown in Fig. 13, the area affected by the landslide is located downstream of the features correlated with the occurrence of the zone of preferential seepage (LRZ-3 and NPA), as discussed in Sect. 4.3. Thus, we interpreted that the loss of stability of the downstream

Fig. 13 Register of the landslide occurred on the downstream slope of the embankment. **a)** Upstream view; **b)** Downstream view; **c)** Top view of the dam highlighting the affected area



slope of the dam can be correlated with the sink identified in the alluvial sand layer.

This correlation strengthens the coherence of the interpretations of the geophysical data that were presented in this study, since both the ER and SP results indicated the existence of the preferential flow path. Also, this result shows the potential of the application of integrated interpretation of geophysical data on the assessment of the efficiency of structural damage correction in geotechnical structures, since the identified flow path can be correlated with the piping process recorded before the data acquisition.

Deficiencies and remarks on data interpretation

Among the main difficulties faced by the authors in obtaining and interpreting the data here presented, one of them was the lack of documentation on the construction of the dam being studied, which limited the search for bibliographic data that could be helpful for better interpretations.

It is important to note that the geophysical survey performed in this study represents the introduction of this methodology in the local context, and that the interpretations presented in this section were aided by research into historical drilling data that provided punctual information along the structure, as well as the data collected during the visual inspection of its surface.

In addition, the existence of geophysical studies prior to the campaign carried out could provide complementary information for obtaining more accurate suggestions about the geotechnical characteristics of the structure in question.

Conclusions

The analysis of our results allowed to conclude that the geophysical survey conducted in the present study proved to be effective for the evaluation of geotechnical conditions and seepage throughout the massif and its foundation layers, fulfilling the objectives of this study. It was possible to delimit surface and deep flow paths occurring in the study area, identifying each phenomenon responsible for its occurrence.

The integrated interpretation of data obtained from the geophysical surveys, together with geotechnical data from previous studies, proved to be an effective tool for better grounded and more precise interpretation of the phenomena presented, confirming the formulated hypotheses, as the SPT data provide reliable information about the constitution and compaction state of the soil mass. In addition, data acquisition by two different methods on the same line profiles provided the necessary redundancy of information required to mitigate possible conflicting interpretations, as both methods are commonly applied to characterize the position and flow of underground water.

The innovations of the paper include the introduction of an alternative dam monitoring methodology into the local context of the area where the study was carried out, incorporating practices commonly applied to large structures in the mining and power generation contexts into the assessment of a small earth dam. In addition, the possibility of applying the proposed methodology to the retroanalysis of the causes of failure in earth structures was shown.

Regarding the safety evaluation of the dam, the results show that although the erosive process caused by piping has been treated, the phenomena responsible for the occurrence

of this process have not been mitigated. In addition, the results show the importance of constant monitoring of geotechnical structures as a tool to avoid structural damage that could lead to their collapse, as the partial slope failure recently occurred between the spillways.

Declarations

This study was financed in part by the Coordenação de Aperfeiçoamento de Pessoal de Nível Superior—Brasil (CAPES)—Finance Code 001. The authors are also grateful to Federal University of Viçosa and Neogeo Geotecnologia Ltda, for providing the equipment, software and personnel necessary for the execution of this project.

Competing of interests The authors declare that they have no known competing financial interests or personal relationships that could have appeared to influence the work reported in this paper.

References

- ANA (Agência Nacional de Águas) (2016) Guia Prático de Pequenas Barragens - Manual do Empreendedor sobre Segurança de Barragens - Volume VIII. Brasília: ANA, p 120
- Andrade LCR (2010) Estudo da influência do meio físico e das atividades antrópicas na qualidade da água na sub-bacia do Córrego Palmital – Viçosa (MG). Universidade Federal de Viçosa, p 154
- Andrades-Filho CO, Rossetti DF, Bezerra FHR, Medeiros WE, Valeriano MM, Cremon EH, Oliveira RG (2014) Mapping neogene and quaternary sedimentary deposits in northeastern Brazil by integrating geophysics, remote sensing and geological field data. *J S Am Earth Sci* 56:316–327. <https://doi.org/10.1016/j.jsames.2014.09.018>
- Associação Brasileira de Geologia de Engenharia (1998) Geologia de engenharia. ABGE, São Paulo, p 587
- Avila-Diaz A, Justino F, Lindemann DS, Rodrigues JM, Ferreira GR (2020) Climatological aspects and changes in temperature and precipitation extremes in Viçosa-Minas Gerais. *An Acad Bras Cienc* 92(2). <https://doi.org/10.1590/0001-3765202020190388>
- Bedrosian PA, Burton BL, Powers MH, Minsley BJ (2012) Geophysical investigations of geology and structure at the Mathis Creek Dam, Truckee, California. *J Appl Geophys* 77:7–20. <https://doi.org/10.1016/j.jappgeo.2011.11.002>
- Bièvre G, Lacroix P, Oxarango L, Goutaland D, Monnot G, Fargier Y (2017) Integration of geotechnical and geophysical techniques for the characterization of a small earth-filled canal dyke and the localization of water leakage. *J Appl Geophys* 139:1–15. <https://doi.org/10.1016/j.jappgeo.2017.02.002>
- Bolève A, Janot F, Revil A, Lafon A, Fry JJ (2011) Localization and quantification of leakages in dams using time-lapse self-potential measurements associated with salt tracer injection. *J Hydrol* 403(3–4):242–252. <https://doi.org/10.1016/j.jhydrol.2011.04.008>
- Camarero PL, Moreira CA (2017) Geophysical investigation of earth dam using the electrical tomography resistivity technique. *REM: Int Eng J* 70(1):47–52. <https://doi.org/10.1590/0370-44672016700099>
- Cardarelli E, Cercato M, di Filippo G (2010) Geophysical investigation for the rehabilitation of a flood control embankment. *Near Surf Geophys* 8:287–296
- Casagrande A (1976) Liquefaction and cyclic deformation of sands - a critical review. Harvard Soil Mechanics Series n° 88. Harvard University, Cambridge, p 55
- Corrêa GF (1984) Modelo de evolução e mineralogia da fração argila dos solos do Planalto de Viçosa. Universidade Federal de Viçosa, MG, p 86
- Corwin RF (1990) The self-potential method for environmental and engineering applications. Geotechnical and environmental geophysics. Tulsa, OK: Society of Exploration Geophysicists. 1.- Review and Tutorial, pp 127–143
- Cruz PT (2004) 100 barragens brasileiras: casos históricos, materiais de construção, projeto. São Paulo: Editora Oficina de textos, p 648
- Daker A (1983) Captação, Elevação e Melhoramento da Água; A água na agricultura. Rio de Janeiro: Freitas Bastos, p 408
- Dalmaschio CF, Barbosa CV, Silva NF (2019) Estudo da aplicação de injeção de cimento em barragem assente sobre solo aluvionar. Universidade Federal de Viçosa. Departamento de Engenharia Civil, Universidade Federal de Viçosa, Viçosa
- Dentith M, Mudge ST (2014) Geophysics for the mineral exploration geoscientist. Cambridge University Press, p 454
- Fell R, Fry JJ (2007) Internal erosion of dams and their foundations. London: Taylor e Francis, pp 1–23. <https://doi.org/10.1201/9781482266146>
- Franco LM, La Terra EM, Panetto LP, Fontes SL (2024) Integrated application of geophysical methods in Earth dam monitoring. *Bull Eng Geol Environ* 83:62. <https://doi.org/10.1007/s10064-024-03551-x>
- Gallas JDF (2005) O método do potencial espontâneo (SP) – Uma revisão sobre suas causas, seu uso histórico e suas aplicações atuais. *Braz J Geophys* 23(2):133–144
- Gandolfo OCB (ed) (2007) Um estudo do imageamento geoeletrico na investigação rasa. Instituto de Geociências, São Paulo, p 234. <https://doi.org/10.11606/T.44.2007.tde-25042008-142218>
- Golebiowski T, Porzucek S, Pasierb B (2016) Ambiguities in geophysical interpretation during fracture detection - case study from a limestone quarry (Lower Silesia Region, Poland). *Near Surf Geophys* 14:371–384. <https://doi.org/10.3997/1873-0604.2016017>
- Grangeia C, Ávila P, Matias M, Ferreira da Silva E (2011) Mine tailings integrated investigations: The case of Rio tailings (Panasqueira Mine, Central Portugal). *Eng Geol* 123(4):359–372. <https://doi.org/10.1016/j.enggeo.2011.10.001>
- Jongmans D, Garambois S (2007) Geophysical investigation of landslides: a review. *Bulletin De La Société Géologique De France, Société Géologique De France* 178(2):101–112
- Kearey P, Brooks M, Hill I (2009) Geofísica de exploração. São Paulo: Oficina de textos, p 438
- Kutzner C (1997) Earth and rockfill dams: Principles of design and construction. Rotterdam: A.A. Balkema, p 250. <https://doi.org/10.1201/9780203758991>
- Lowrie W (2007) Fundamentals of geophysics, second edition. Cambridge University Press, p 392
- Marques EAG (2008) Relatório técnico de Mapeamento Geológico da Sub-Bacia do Ribeirão São Bartolomeu (MG). Technical report. p 86
- Medeiros AKA, Córdoba VC (2020) Stratigraphic analysis of Ponta do Mel carbonate platform, Albian- Cenomanian in Potiguar Basin, NE of Brazil. *J S Am Earth Sci* 102:12
- Minette E (2015) COMISSÃO NOMEADA PELO ATO 00053/2015/PAD DE 05/06/2015: Relatório técnico. Universidade Federal de Viçosa, Technical report
- Netto LG, Malagutti Filho W, Gandolfo OCB (2020) Detection of seepage paths in small earth dams using the self-potential method (SP). *REM: Int Eng J* 73(3):303–310. <https://doi.org/10.1590/0370-44672018730168>
- Oh S, Sun C-G (2008) Combined analysis of electrical resistivity and geotechnical SPT blow counts for the safety assessment of fill dam. *Environ Geol* 54:31–42. <https://doi.org/10.1007/s00254-007-0790-y>

- Panthulu TV, Krishnaiah C, Shirke JM (2001) Detection of seepage paths in earth dams using self-potential and electrical resistivity methods. *Eng Geol* 59:281–295. [https://doi.org/10.1016/S0013-7952\(00\)00082-X](https://doi.org/10.1016/S0013-7952(00)00082-X)
- Pazzi V, Morelli S, Fanti R (2019) A Review of the Advantages and Limitations of Geophysical Investigations in Landslide Studies. *Int J Geophys* 2019:27. <https://doi.org/10.1155/2019/2983087>
- Raffek MABM (2016) Predicting standard penetration test (SPT-N) value from electrical resistivity result. Monografia. Universiti Teknologi PETRONAS, Seri Iskandar, Perak, Malásia
- Raji WO, Adedoyin DO (2019) Dam safety assessment using 2D electrical resistivity geophysical survey and geological mapping. *J King Saud Univ Sci* 32(1):1123–1129. <https://doi.org/10.1016/j.jksus.2019.10.016>
- Reynolds JM (2011) An introduction to applied and environmental geophysics, 2nd edn. John Wiley & Sons, West Sussex, p 696
- Robbins AB, Griffiths DV (2018) Internal erosion of embankments: A review and appraisal. *Rocky Mountain Geo-Conference 2018 GPP 12*. pp 61–75. <https://doi.org/10.1061/9780784481936.005>
- Rocha SF (2015) Implantação De Um Sistema De Filtração Em Margem E Avaliação Hidrogeológica Da Interação Lago – Aquífero. Departamento de Engenharia Civil, Universidade Federal de Viçosa, Viçosa, p 115
- Rocha DCG, Braga MAS, Rodrigues CT (2019) Geophysical methods for br tailings dam research and monitoring in the mineral complex of Tapira - Minas Gerais, Brazil. *Braz J Geophys* 37(3):275–289. <https://doi.org/10.22564/rbgf.v37i3.2007>
- Roy O (1962) Ambiguity in geophysical interpretation. *Geophysics* 27(1):90–99. <https://doi.org/10.1190/1.1438985>
- Telford WM, Geldart LP, Sheriff RE (1990) Applied geophysics, second ed. Cambridge: Cambridge University Press, p 792. <https://doi.org/10.1017/CBO9781139167932>
- UFV (Universidade Federal de Viçosa) (2018) Injeção de Calda de Cimento - Barragem – Ufv: Technical report, p 20
- UFV (Universidade Federal de Viçosa) (2021) Estação Climatológica Principal de Viçosa. Boletim meteorológico 2021. Technical report. Departamento de Engenharia Agrícola, Viçosa, p 169